Ti-Implanted Nanoscale Layers for the Chloramphenicol Photocatalytic Decomposition

O. V. Sanzhak, D. V. Brazhnyk, V. V. Honcharov, and V. A. Zazhigalov

1 Introduction

Pollution of the environment is an acute problem today. At the same time, important factors are not only emissions from transport and energetics, but also waste pollution from various industries, including pharmaceuticals [1–6].

Photocatalysis is one of the effective solutions to this problem. In particular, photocatalysts were used in the study of chloramphenicol utilization problems [7–11]. Moreover, although catalysts with an active ingredient based on silver have proven themselves well [12], the search for active compositions with cheaper components is in progress. Titanium oxides can be considered promising in this regard [3, 8, 9, 13, 14].

Due to a number of disadvantages of existing titanium (low activity in the visible light, use in the form of a solution, etc. [15, 16]) one of the main issues is the structure and composition of existing titanium photocatalysts.

Given the above, we can assume that the most optimal designs of photocatalysts for operation under irradiation conditions will be supported systems [8, 17, 18]. In addition, an important factor is the dimensionality of the structure. It is shown that nanoscale structures achieve a significant effect in catalysis [7, 9, 11, 19, 20].

Therefore, to obtain effective photocatalysts, it is necessary to determine the preparation technology and composition of the supported system.

O. V. Sanzhak · D. V. Brazhnyk · V. A. Zazhigalov
Institute for Sorption and Problems of Endoecology NAS Ukraine, Kyiv, Ukraine
e-mail: zazhigal@ispe.kiev.ua

V. V. Honcharov (✉)
State Establishment "Lugansk State Medical University", Rubizhne, Ukraine
e-mail: milostiprosim@i.ua

O. Fesenko and L. Yatsenko (eds.), *Nanomaterials and Nanocomposites, Nanostructure Surfaces, and Their Applications*, Springer Proceedings in Physics 263, https://doi.org/10.1007/978-3-030-74741-1_7

Supports from metallic foil have advantages compared with glass, ceramics, etc. They are strong, stable in many environments, conduct heat well, and durable. In addition, their plasticity allows to creating of catalysts of almost any shape.

As a method of synthesis supported catalysts, ion-plasma technologies have a number of advantages [19, 21–23]. In particular, ionic implantation technology is attractive for the treatment of catalytic carriers [24–26]. It permits to obtain a thin surface layer active component due to its bombardment by target ions with significant energies. Due to the emission of surface atoms and mixing with implanted ions, new compounds are formed and the surface layer of the sample is strengthened. In contrast to the traditional applied layers, the obtained modified surface has significant strength and heat resistance. Therefore, the structural properties of implants obtained by implanting titanium ions in steel and aluminum were studied. Some samples were oxidized at different temperatures and investigated in the reaction of chloramphenicol photodegradation.

2 The Experimental Part

The detail of synthesis technology of nanoscaled modified layers is described in [19, 27]. Stainless steel foil (100 μm) and aluminum foil (50 μm) were treated by titanium ions according to this method. The samples are marked: Ti/SS and Ti/Al accordingly. After implantation, some of the samples were calcinated on air at different temperatures (200, 300, 400, 500, 600 °C). Calcination time of the sample at each temperature was equal to two hours.

Methods SEM (scanning electron microscopy) and EDXS (energy-dispersive X-ray spectroscopy) were used to determine the qualitative and quantitative composition of the samples. The research was performed using scanning electron microscope Tescan Vega3 LMU and an energy-dispersive X-ray microanalyzer (Oxford Instruments Aztec ONE with X-MaxN20 detector) at the Center for Collective Use "Laboratory of Materials Science of Intermetallic Compounds" at Lviv National University named after Ivan Franko.

Scanning of the surface of the samples (sections) was carried out using an electron beam (generated by a gun W-thermocathode) with a diameter of several nanometers and accelerated voltage of ~25 kV. The maximum resolution reaches 30.0 Å at high vacuum and voltage of 30 kV (increase ~1,000,000 times). The operating distance from the gun to the sample in the SEM method varies from the required increase, for sections of metal alloys is 15–20 mm. The microscope is designed to study samples in high and variable vacuum. At high vacuum ($9.9–10^{-3}$ Pa), it is possible to investigate conductive samples (typical alloys of intermetallics), partially conductive samples (semiconductor alloys, films, crystals) or non-conductive samples (polymers, objects of biological origin, etc.) with a sprayed layer of conductive coatings (such as carbon or gold). Variable vacuum is more often used in the study of nano-objects with a developed surface. The microscope is equipped with two detectors SE and BSE. In the SE-detector mode ("secondary electrons"), the surface condition (topographic

contrast) of the sample can be estimated, and in the BSE-detector mode ("reflected secondary electrons") phases can be identified based on the contrast by the average atomic number (the phase with more electrons will be colored lighter than the phase based on elements with a smaller sequence number). The range of quantitative determination of elements is from Be to Cf. The optimal working distance from the gun to the sample in EDRS methods is 15–17 mm for conductive samples.

Arrays of experimental intensities and angles from the studied samples were obtained on an automatic diffractometer STOE STADI P (manufactured by STOE & Cie GmbH, Germany). It is equipped with a linear position-precision PSD detector according to the scheme of modified Guine geometry and the method of passing bending (CuKα1 radiation; concave Ge monochromator (111) of Johann type; range of angles 2θ was $4.000 \leq 2\theta \leq 99.985°$ with a step of 0.015° 2θ; step of the detector was equal to 0.480° (2θ).

The detail of the samples study by SAXS and XPS methods was reported in [19, 27, 28]. The procedure of determination of elements distribution in surface layer by XPS method was described in [27].

The photocatalytic properties of the samples in degradation of chloramphenicol (50 threshold limit values (TLV)) was determined under visible and UV irradiation. The study was carried out in a cylindrical reactor (9 cm diameter) with a wall-placed 10 cm height sample (implantation on both sides of the foil) and immersed thermostatically controlled radiation source. The source of radiation (high-pressure mercury or sodium lamps were used) was placed in reactor center, which permits to implement the investigation in both UV and visible range. The reaction products were analyzed on a SelmiChrom-2 gas chromatograph equipped with a FID on a stainless steel column (length 1 m, diameter 3 mm) filled with Porapak Q.

3 Results and Discussion

The data obtained by XRD method (Figs. 1 and 2) demonstrate the presence of (111) (200) and (220) planes austenite reflexes (initial stainless steel) in diffractograms of all synthesized samples with implanted titanium. This fact coincides with the results obtained in the work [27].

A similar situation is observed for samples on aluminum foil (Figs. 3, and 4).

The lack of reflexes other than the original ones can be explained by the fact that ionic implantation does not create distinct crystalline structures in the surface layer.

From the SEM data (cross section) [19, 27], it is known that the stainless steel surface after titanium implantation has the new layer (thickness of this layer is near to 80 nm).

The results of XPS study demonstrate the presence of titanium (target ions), oxygen (from air), and nitrogen (from plasma of the ion source) in this nanolayer [27] and the formation of amorphous titanium oxynitride and nitride of titanium in this layer on stainless steel surface as result of titanium implantation. It was shown [27] that treatment of this sample at 600 °C led to formation of titanium oxide in

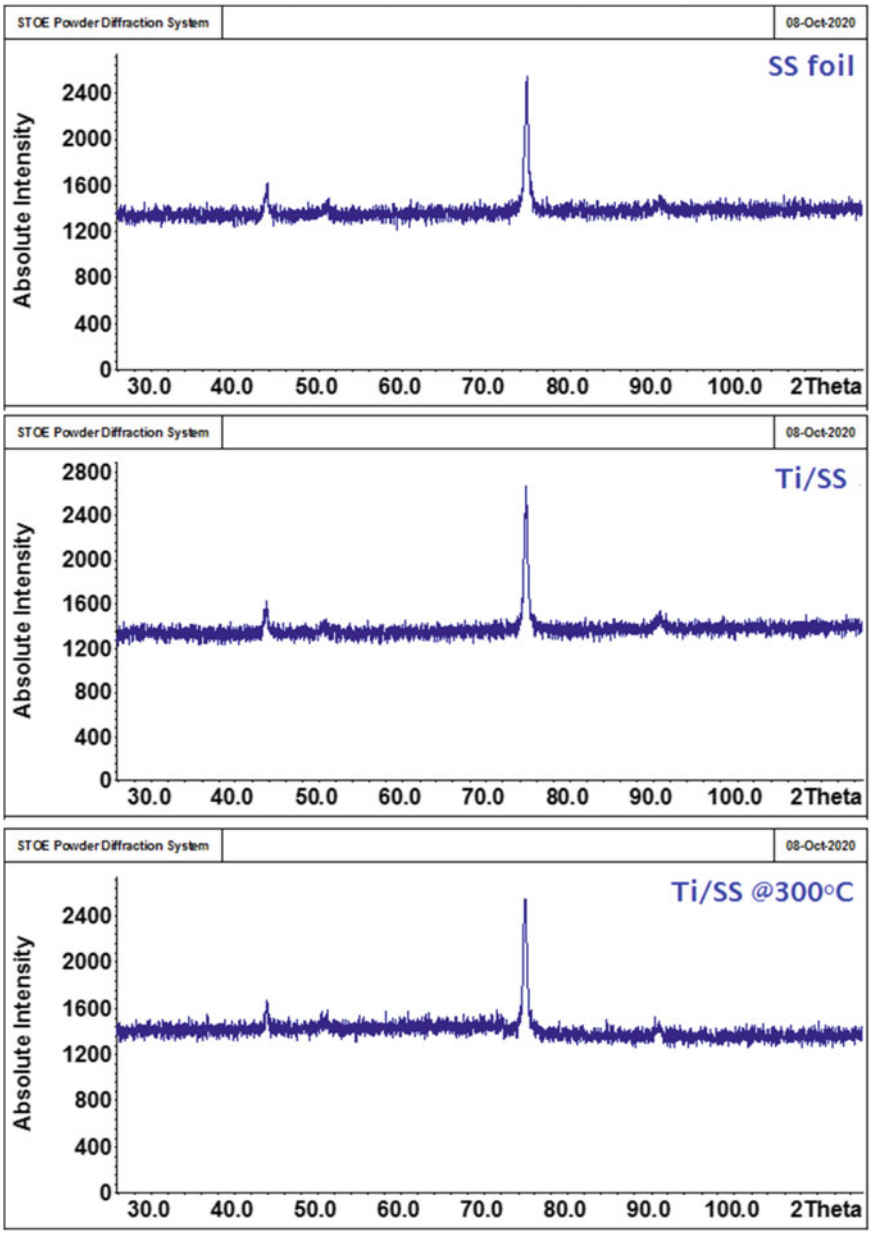

Fig. 1 Data of XRD analysis for initial SS foil, Ti/SS, and Ti/SS oxidized at 300 °C

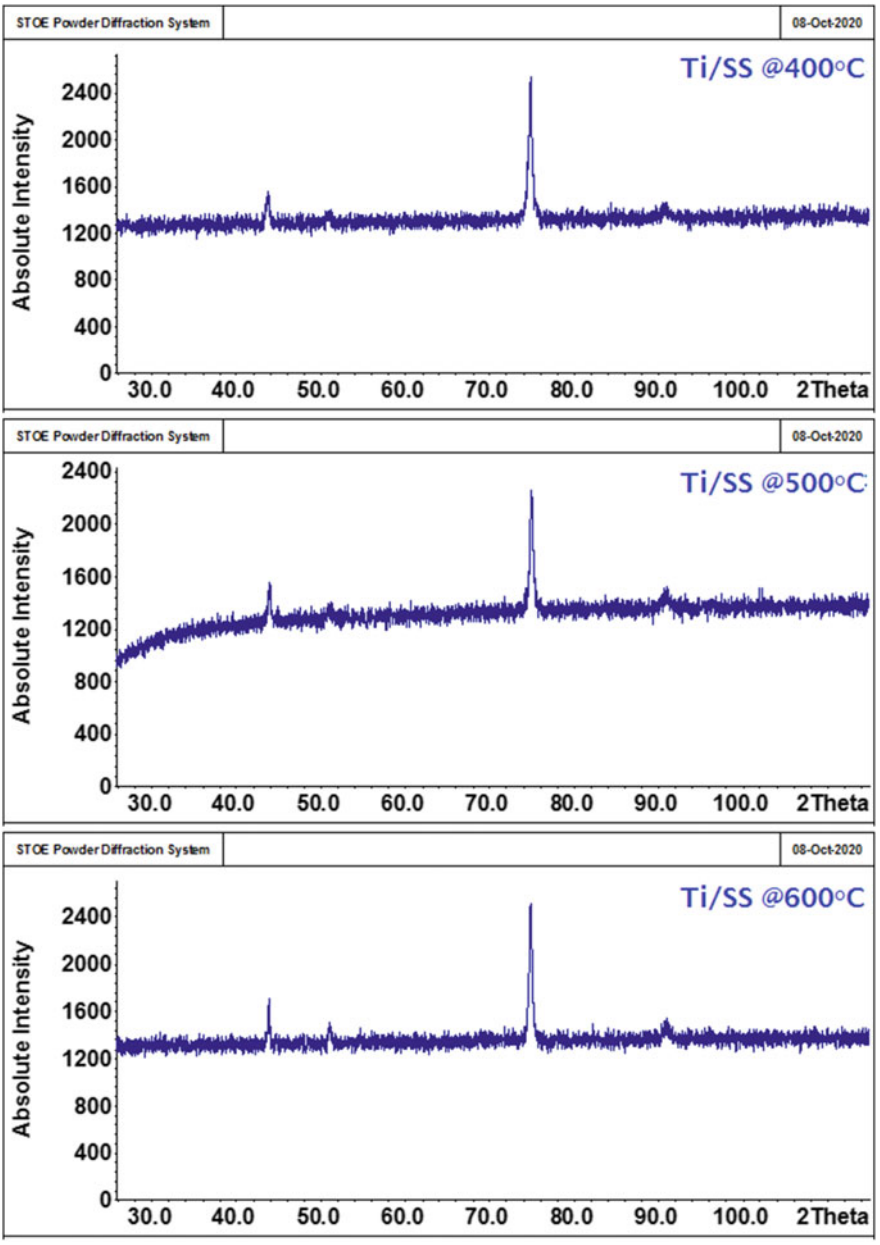

Fig. 2 data of XRD analysis for Ti/SS oxidized at 400, 500, and 600 °C

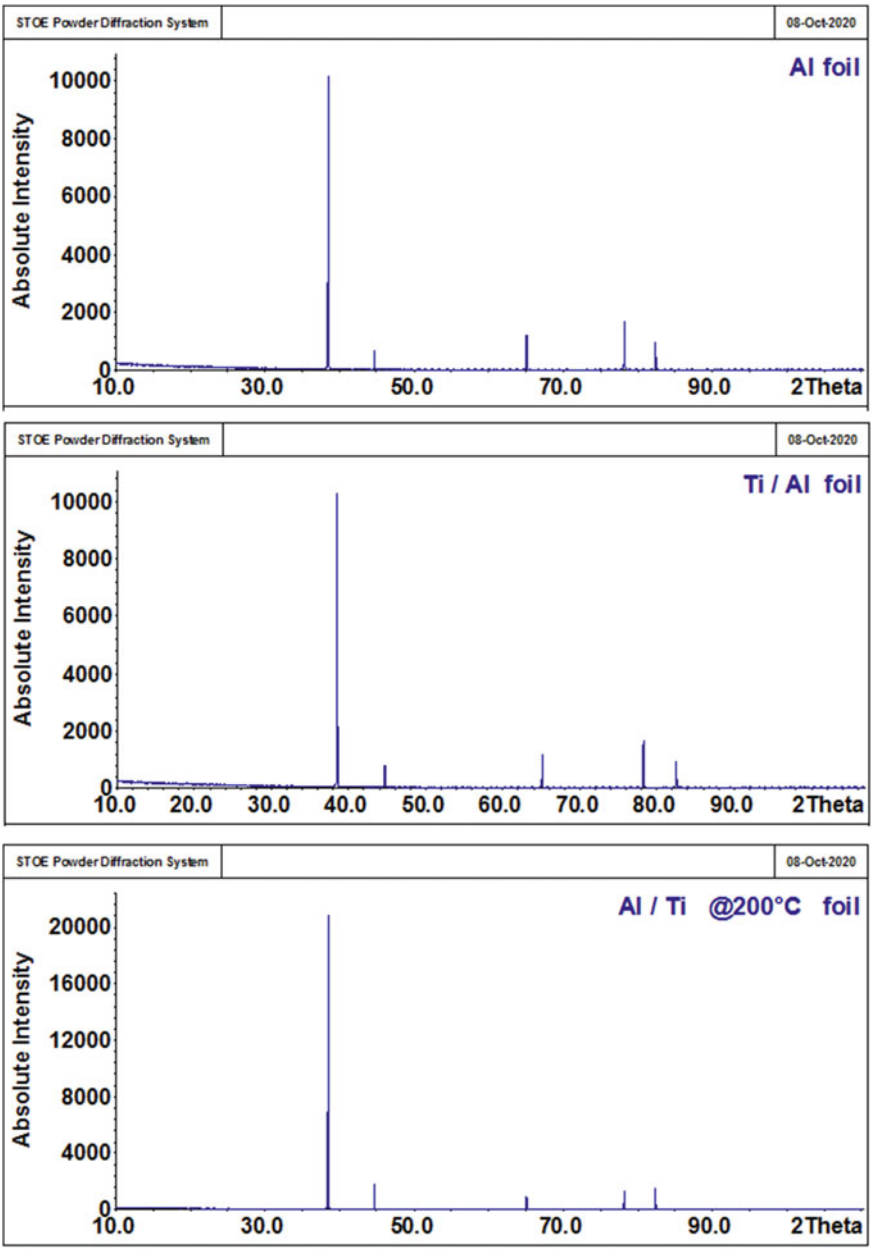

Fig. 3 Data of XRD analysis for initial Al foil, Ti/Al, and Ti/Al oxidized at 200 °C

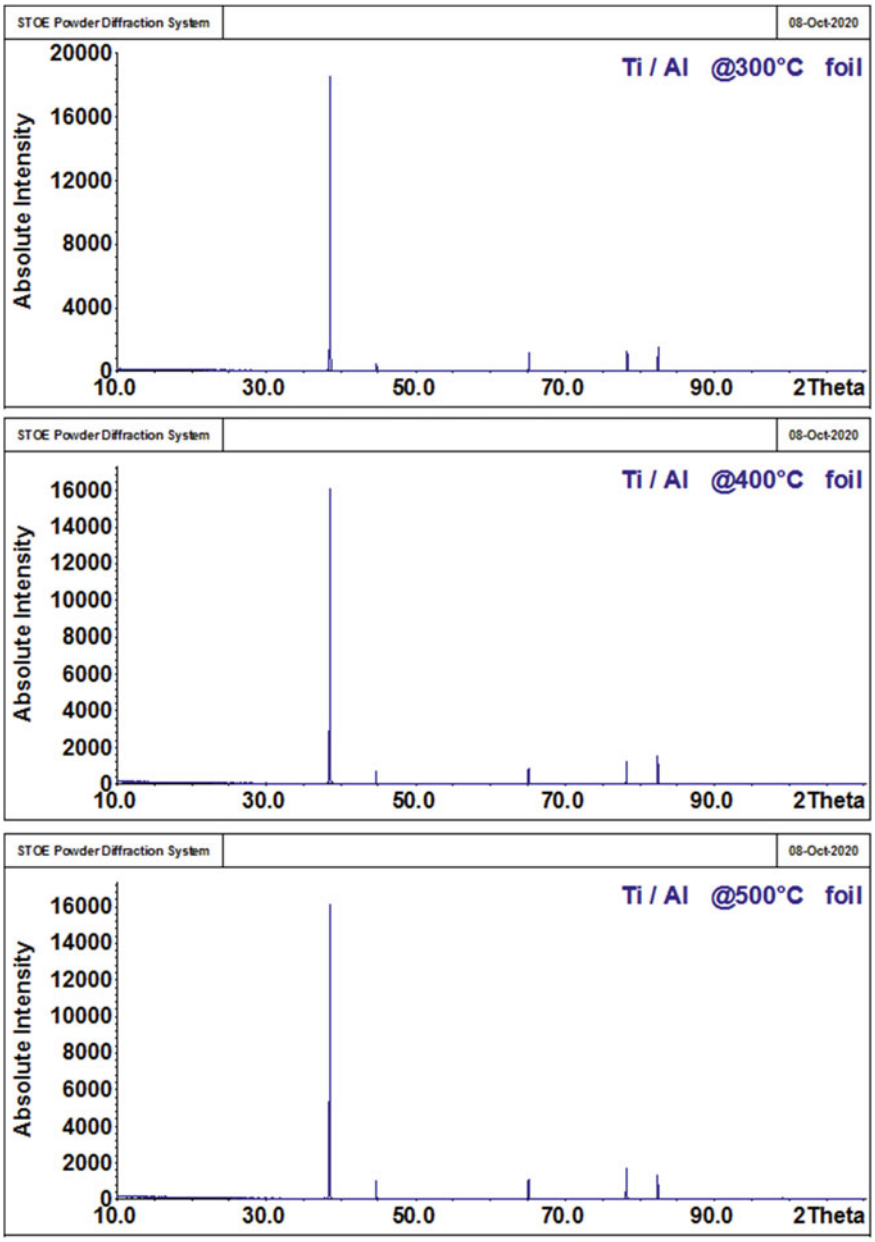

Fig. 4 Data of XRD analysis for Ti/Al oxidized at 300, 400, and 500 °C

this surface layer. The influence of other temperatures of the sample treatment on its properties was not studied. Therefore, an elemental analysis and morphology of the surface layer was performed using SEM and EDXS.

The results (Fig. 5) of the study of morphology (SEM) show that the treatment of the steel sample with titanium ions leads to the severity of the relief. Smaller formations are smoothed, and larger ones are enlarged. After annealing of the samples, the microgeometry changes again—there is a smoothing and averaging of defects. With increasing of the treatment temperature, this effect increases.

On initial sample of aluminum foil (Fig. 6), the defects are visible in the form of stripes, which is the result of production technology. After implantation of titanium, as well as for steel foil, there is an expression of a relief, which is smoothed at oxidation, leaving only technological strips.

The similarities in the behavior of implants on different media confirm the results of EDXS.

EDXS analysis of aluminum-based implants (Fig. 7) shown in the original sample only the components that must be according to the production technology. After implantation, the amount of oxygen in the samples increases and nitrogen appears which enters with the ion stream from the ion source plasma.

It is determined that after oxidation with a temperature of 500 °C (Fig. 7c) only the ratio of nitrogen–oxygen changes in favor of the latter.

Similarly, the composition of the sample synthesized by processing steel foil is changed (Fig. 8).

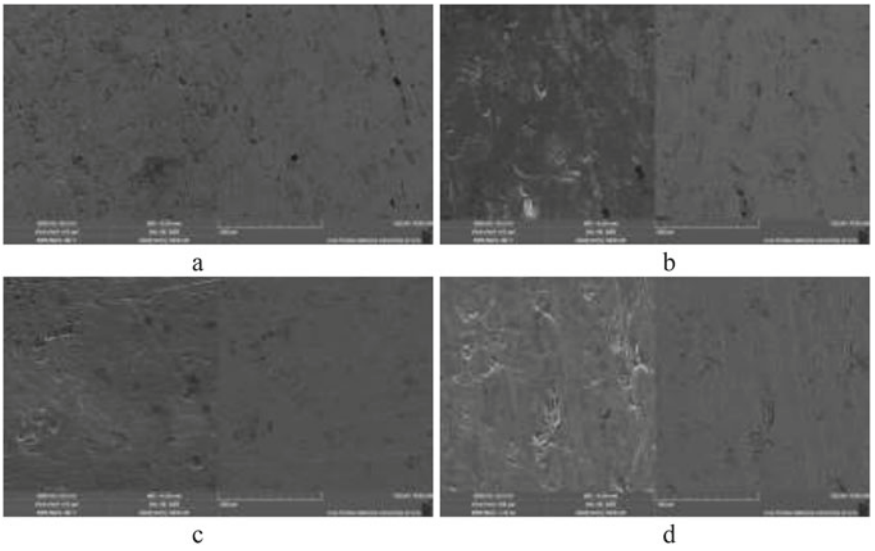

Fig. 5 Data of SEM investigation of initial steel SS (**a**), sample Ti/SS (**b**) and after its temperature treatment under 300 °C (**c**) and 400 °C (**d**)

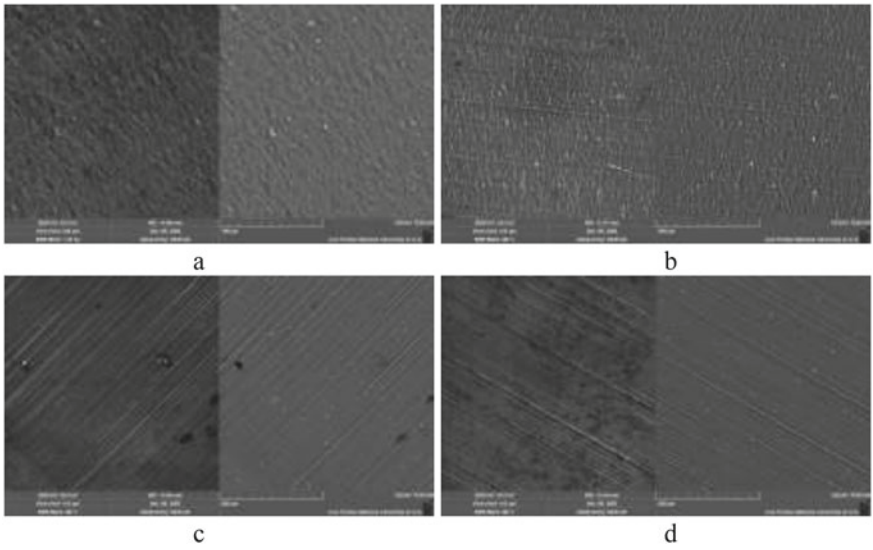

Fig. 6 Data of SEM investigation of initial foil Al (**a**), sample Ti/Al (**b**), and after its temperature treatment under 200 °C (**c**) and 300 °C (**d**)

The original sample (Fig. 8a) corresponds to the standard composition of the components.

During processing, it receives oxygen (Fig. 8b), which the amount increases after oxidation (Fig. 8c).

The obtained results of the samples investigation and the literature data [19, 27] show the perspective of the study of the synthesized implants in the reaction of chloramphenicol (CAP) decomposition (Fig. 9).

The obtained results of photocatalytic activity of implants with titanium ions demonstrate that the chloramphenicol degradation at UV irradiation (all samples were inactive in visible light irradiation) proceed with an offset toward the visible range. Moreover, the magnitude of this shift depends on the exposure time of the sample (Fig. 9). So, it is possible to suppose that photocatalytic activity of the catalysts prepared by ionic implantation of titanium on stainless steel depend on surface composition and morphology, which allows the selection of the appropriate catalyst.

4 Conclusions

The samples were synthesized on aluminum and steel carriers by ion implantation. It is shown that there are no newly formed crystalline structures in the surface layer of the support samples and this state is observed for oxidized carriers as well. The formation of surface nanolayer of implanted titanium was established.

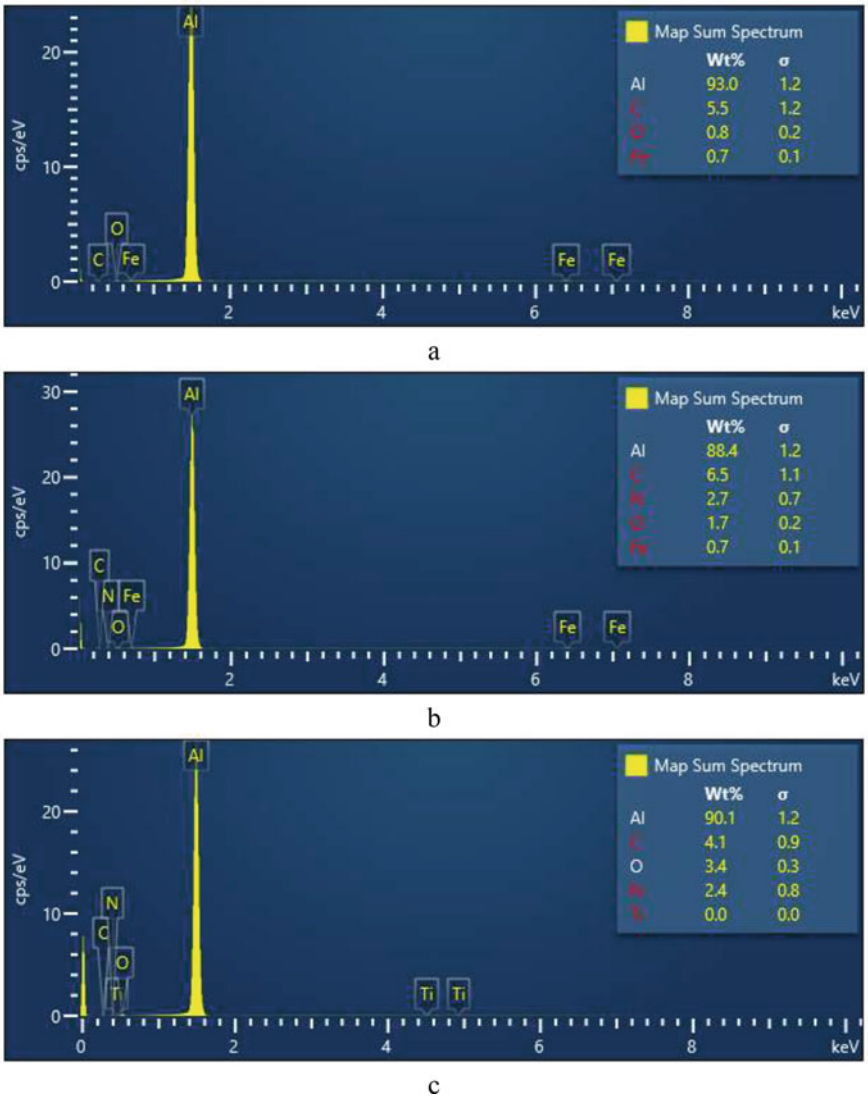

Fig. 7 Data of EDXS analysis of initial foil Al (**a**), sample Ti/Al (**b**), and after its temperature treatment under 500 °C (**c**)

It was found that the samples synthesized on stainless steel by ionic implantation change their morphology during oxidation in the same way as the samples on aluminum foil. It is shown that the nature of changes in surface composition for samples on different supports is similar. It was found that the implants show some photocatalytic activity in the decomposition reaction of chloramphenicol.

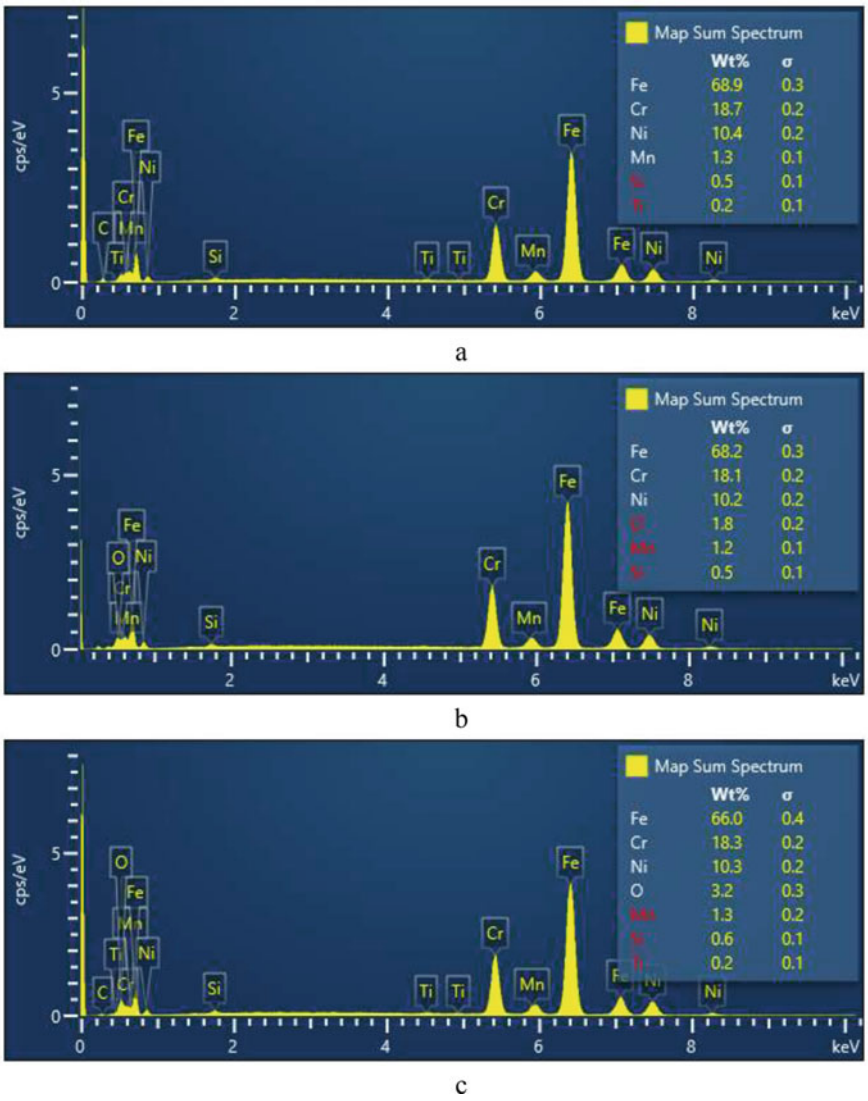

Fig. 8 Data of EDXS analysis of initial foil SS (**a**), initial sample Ti/SS (**b**), and after its temperature treatment under 500 °C (**c**)

Thus, ionic implantation has significant potential as a technology for the synthesis of photocatalysts, which is relevant for environmental catalysis, energetics, pharmaceutical industry and more.

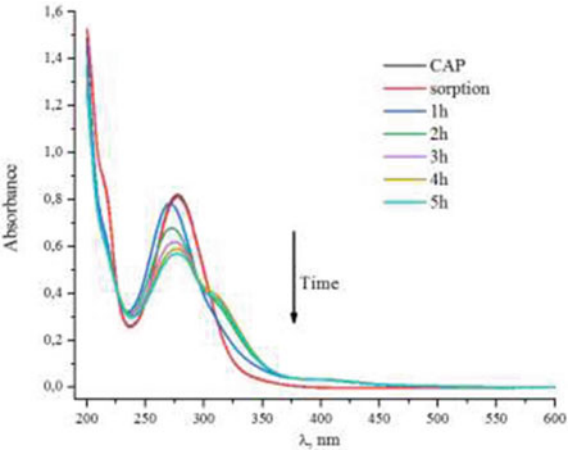

Fig. 9 Photocatalytic degradation of the chloramphenicol on the Ti/SS sample treated at 200 °C

Acknowledgements The investigations were realized with partial financial support of NAS of Ukraine Fundamental Programme "Fine Chemicals," Project 20-(14-16).

References

1. Homem V, Santos L (2011) Degradation and removal methods of antibiotics from aqueous matrices—a review. J Environ Manage 92:2304–2347
2. Michael I, Rizzo L, McArdell CS et al (2013) Urban wastewater treatment plants as hotspots for the release of antibiotics in the environment: a review. Water Res 47:957–995
3. Chatzitakis A, Berberidoua C, Paspaltsisb I et al (2008) Photocatalytic degradation and drug activity reduction of chloramphenicol. Water Res 42:386–394
4. Akimenko YuV, Kazeev KSh, Kolesnikov SI et al (2013) Ecological consequences of pollution of soils antibiotics. Izvestiya Samarskogo nauchnogo tsentra Rossiyskoy akademii nauk 15(3):1196–1199
5. Sarmah AK, Meyer MT, Boxall ABA (2006) A global perspective on the use, sales, exposure pathways, occurrence, fate and effects of veterinary antibiotics (VAs) in the environment. Chemosphere 65:725–759
6. Dolina LF, Savina OP (2018) Water cleaning from residues of medicinal preparations. Nauka ta prohres transportu. Visnyk Dnipropetrovs'koho natsional'noho universytetu zaliznychnoho transportu 3(75):36–51
7. Kulkarnia RM, Malladi RS (1989) Hanagadakara MS (20018) Ba-ZnO nanoparticles for photocatalytic degradation of chloramphenicol. AIP Conf Proc 020026:1–9
8. Baezab B, Lizamaa C, Caneob C et al (2007) Factorial design for the photodegradation of chloramphenicol with immobilized TiO_2. J Adv Oxid Techno 10(2):411–414
9. Palma TL, Vieira B, Nuneset J et al (2020) Photodegradation of chloramphenicol and paracetamol using PbS/TiO_2 nanocomposites produced by green synthesis. J Iran Chem Soc 17:2013–2031
10. Csay T, Racz G, Takacs E et al (2012) Radiation induced degradation of pharmaceutical residues in water: Chloramphenicol. Radiat Phys Chem 81:1489–1494
11. Qin Xu, Song Z, Ji S et al (2019) The photocatalytic degradation of chloramphenicol with electrospun Bi2O2CO3-poly(ethylene oxide) nanofibers: the synthesis of crosslinked polymer, degradation kinetics, mechanism and cytotoxicity. RSC Adv 9:29917–29926

12. Ma Y, Dongyao Wu, Liu C et al (2018) Preparation of Fe-Ag3VO4/GO composite photocatalyst for enhanced photodegradation of chloramphenicol. ICACEES 2018:199–203
13. Malato S, Fernandez-Ibanez P, Maldonado et al (2009) Decontamination and disinfection of water by solar photocatalysis: recent overview and trends. Cataly Today 147:1–59
14. Thompson TL, Yates JT (2006) Surface science studies of the pho-toactivation of TiO_2 new photochemical processes. Chem Rev 106:4428–4453
15. Hiroshi I, Yuka W, Kazuhito H (2003) Carbon-doped anatase TiO_2 powders as a visible-light sensitive photocatalyst. Chem Lett 32(8):772–773
16. Lin X, Rong F, Fu D, Yuan C (2012) Enhanced photocatalytic activity of fluorine doped TiO_2 by loaded with Ag for degradation of organic pollutants. Powder Tech 219:173–178
17. Ang YS, Tinia IMG., Suraya AR (2010) Immobilisation of titanium dioxide onto supporting materials in heterogeneous photocatalysis—a review. Appl Catal A General 389:1–8
18. Rachel A, Subrahmanyan M, Boule P (2002) Comparison of photocatalytic efficiencies of TiO2 in suspended and immobilised form for photocatalytic degradation of nitrobenzenesulfonic acids. Appl Catal B Environm 37:301–308
19. Honcharov V, Zazhigalov V, Sawlowicz Z, Socha R, Gurgol J (2017) Structural, catalytic, and thermal properties of stainless steel with nanoscale metal surface layer. In: Fesenko O, Yatsenko L (eds) Nanophysics, nanomaterials, interface studies, and applications. NANO 2016. Springer Proceedings in Physics, vol 195. Springer, Cham, pp 355–364
20. Chena J, Li Y, Li Z et al (2004) Production of COx-free hydrogen and nanocarbon by direct decomposition of undiluted methane on Ni–Cu–alumina catalysts. Appl Catal A 269:179–186
21. Magali BK, Sven GJ (1996) A review of the use of plasma techniques in catalyst preparation and catalytic reactions. Appl Catal A 147:1–21
22. Liu CJ, Vissokov G, Jang BWL (2002) Catalyst preparation using plasma technologies. Catal Today 72:173–184
23. Durme JV, Dewulf J, Leys C et al (2008) Combining non-thermal plasma with heterogeneous catalysis in waste gas treatment: a review. Appl Catal B 78:324–333
24. June KT, Jeong-Gil K, Ho-Young L et al (2014) Modification of optical and mechanical surface properties of sputter-deposited aluminum thin films through ion implantation. Int J Precis Eng Manuf 15(5):889–894
25. Kalin BA (2001) Radiatsionno-puchkovyye tekhnologii obrabotki konstruktsionnykh materialov. Fiz Khim Obrab Mater 4:5–16
26. Wang H, Zhang S, Yu D et al (2011) Surface modification of (Tb, Dy)Fe_2 alloy by nitrogen ion implantation. J Rare Earths 29(9):878–882
27. Zazhigalov VA, Honcharov VV, Bacherikova IV, Socha R, Gurgul J (2018) Formation of nanodimension layer of catalytically active metals on stainless stail surface by ionic implantation. Theor Experim Chem 34(2):128–137
28. Zazhigalov VA, Honcharov VV (2014) Formirovaniye nanorazmernogo pokrytiya na stali 12H18N10T pri ionnoy implantatsii. Metallofizika i Noveishie Tekhnologii 6(36):757–766